JPET Fast Forward. Published on November 30, 2011 as DOI: 10.1124/jpet.111.188136

#188136

TITLE PAGE

Development of Angiotensin IV Analogs as Hepatocyte Growth Factor/Met Modifiers

Leen H. Kawas, Alene T. McCoy, Brent J. Yamamoto, John W Wright, Joseph W. Harding

Department of Veterinary and Comparative Anatomy, Pharmacology, and Physiology, Washington State University, Pullman, WA-LHK, ATM, BJY, JWW, JWH

Department of Psychology, Washington State University, Pullman, WA-JWW, JWH

Program in Pharmacology and Toxicology Washington State University, Pullman, WA-LHK, AM, BJY, JWH

JPET Fast Forward. Published on November 30, 2011 as DOI: 10.1124/jpet.111.188136
This article has not been copyedited and formatted. The final version may differ from this version.

RUNNING TITLE PAGE

a) Running title page: Anti-Met/cancer activity of HGF dimerization domain mimics

b) Corresponding author:
Dr. Joseph W Harding
Department of Veterinary and Comparative Anatomy, Pharmacology, and Physiology
PO Box 6520
Washington State University
Pullman, WA 99164-6520 USA
Phone: 509 335-7927
FAX: 509 335-4652
E-mail: hardingj@vetmed.wsu.edu

c) Number of text pages: 30

Number of figures: 8

Number of References: 40

Word count: Abstract-232; Introduction-676; Discussion-681

List of non-standard abbreviations:

HEK293: Human embryonic kidney cells 293; MDCK: Madin Darby canine kidney cells; HGF: Hepatocyte Growth Factor; Bis-Tris: 2-[bis(2 hydroxyethyl)amino]-2-(hydroxymethyl)propane-1,3-diol ; ψ-(CH_2-NH_2): reduced peptide bond; BS3: Bissulfosuccinimidyl suberate; MSP: Macrophage Stimulating Protein; Nle^1-AngIV: Nle-Tyr-Ile-His-Pro-Phe

d) Recommended section assignment: Drug discovery and translational medicine.

JPET Fast Forward. Published on November 30, 2011 as DOI: 10.1124/jpet.111.188136
This article has not been copyedited and formatted. The final version may differ from this version.

ABSTRACT

The 6-AH family [D-Nle-X-Ile-NH-$(CH_2)_5$-$CONH_2$; where X= various amino acids] of Angiotensin IV analogs, bind directly to Hepatocyte Growth Factor (HGF) and inhibit HGF's ability to form functional dimers. The metabolically stabilized 6-AH family member, D-Nle-Tyr-Ile-NH-$(CH_2)_5$-$CONH_2$, had a $t_{1/2}$ in blood of 80 min compared to the parent compound Norleual (Nle-Tyr-Leu-Ψ-$(CH_2$-$NH_2)^{3-4}$-His-Pro-Phe), which had a $t_{1/2}$ in blood of < 5 min. 6-AH family members were found to act as mimics of the dimerization domain of HGF (hinge region), and inhibited the interaction of an HGF molecule with a ^{3}H-hinge region peptide resulting in an attenuated capacity of HGF to activate its receptor Met. This interference translated into inhibition of HGF-dependent signaling, proliferation, and scattering in multiple cell types at concentrations down into the low picomolar range. We also noted a significant correlation between the ability of the 6-AH family members to block HGF dimerization and inhibition of the cellular activity. Further, a member of the 6-AH family with cysteine at position 2, was a particularly effective antagonist of HGF-dependent cellular activities. This compound suppressed pulmonary colonization by B16-F10 murine melanoma cells, which are characterized by an overactive HGF/Met system. Together these data indicate that the 6-AH family of AngIV analogs exert their biological activity by modifying the activity of the HGF/Met system and offer the potential as therapeutic agents in disorders that are dependent on or possess an over-activation of the HGF/Met system.

JPET Fast Forward. Published on November 30, 2011 as DOI: 10.1124/jpet.111.188136
This article has not been copyedited and formatted. The final version may differ from this version.

INTRODUCTION

The multifunctional growth factor hepatocyte growth factor (HGF) and its receptor Met are important mediators for mitogenesis, motogenesis, and morphogenesis in a wide range of cell types (Birchmeier et al., 2003) including epithelial (Kakazu et al., 2004), endothelial (Kanda et al., 2006), and hematopoietic cells (Ratajczak et al., 1997), neurons (Thompson et al., 2004), melanocytes (Halaban et al., 1992), and hepatocytes (Borowiak et al., 2004). Furthermore, dysregulation of the HGF/Met system often leads to neoplastic changes and to cancer (in both human and animal) where it contributes to tumor formation, tumor metastasis, and tumor angiogenesis (Christensen et al., 2005; Liu et al., 2008). Over-activation of this signaling system is routinely linked to poor patient prognosis (Liu et al., 2010). Therefore molecules that inhibit the HGF/Met system can be expected to exhibit anti-cancer activity and attenuate malignant and metastatic transformations.

HGF is a vertebrate heteromeric polypeptide growth factor with a domain structure that closely resembles the proteinases of the plasminogen family (Donate et al., 1994). HGF consists of seven domains: an amino terminal domain, a dimerization-linker domain, four kringle domains (K1-K4), and a serine proteinase homology (SPH) domain (Lokker et al., 1992; Chirgadze et al., 1999). The single chain pro-polypeptide is proteolytically processed by convertases to yield a mature α (heavy chain 55 KDa), and β (light chain 34 KDa) heterodimer, which are bound together by a disulfide link (Stella and Comoglio, 1999; Birchmeier et al., 2003; Gherardi et al., 2006). In addition to proteolytic processing, HGF requires dimerization to be fully activated (Lokker et al.,

1992; Chirgadze et al., 1999; Youles et al., 2008). Several reports have shown that HGF forms dimers and/or multimers, which are arranged in a head-to-tail orientation, prior to its interaction with Met (Gherardi et al., 2006). The dimer interface, which encompasses the inter-domain linker amino acids (K122, D123, Y124, I125, R126, and N127) is referred to as the hinge region (Gherardi et al., 2006; Youles et al., 2008). Although both pre-pro-HGF and the active disulfide-linked heterodimer bind Met with high affinity, it is only the heterodimer that is capable of activating Met (Lokker et al., 1992; Sheth et al., 2008).

Recent studies from our laboratory (Yamamoto et al., 2010) have shown that picomolar concentrations of the AngIV analog, Norleual (Nle-Tyr-Leu-ψ-$(CH_2\text{-}NH_2)^{3\text{-}4}$-His-Pro-Phe), are capable of potently inhibiting the HGF/Met system and bind directly to the hinge region of HGF blocking its dimerization (Kawas et al., 2011). Moreover, a hexapeptide representing the actual hinge region possessed biochemical and pharmacological properties identical to Norleual's (Kawas et al., 2011). The major implication of those studies was that molecules, which target the dimerization domain of HGF, could represent novel and viable anti-cancer therapeutics. Additionally, these data support the development of such molecules using Norleual and/or the Hinge peptide as synthetic templates.

Despite its marked anti-cancer profile Norleual is highly unstable making its transition to clinical use problematic. Thus a family of metabolically stabile Ang IV-related analogs has been developed in our laboratory, which are referred to here as the 6-AH family because of 6-amnio hexanoic amide substituted at the C-terminal position.

This substitution along with D-norleucine at the N-terminal enhances the metabolic resistance of family members.

Here we demonstrate that 6-AH family members have superior metabolic stability when compared to Norleual, bind to HGF with high affinity, and act as hinge region mimics; thus preventing HGF dimerization and activation. This interference translates into inhibition of HGF-dependent signaling, proliferation, and scattering in multiple cell types at concentration in the picomolar range. A positive correlation was evident between the ability to block dimerization and the inhibition of the cellular outcomes of HGF activation. Finally D-Nle-Cys-Ile-NH-$(CH_2)_5$-$CONH_2$, a member of the 6-AH family suppressed pulmonary colonization by B16-F10 murine melanoma cells, which are characterized by an overactive HGF/Met system.

These studies highlight the ability of AngIV-like molecules to bind to HGF, block HGF dimerization, and inhibit the HGF/Met system. Moreover, these data encourage the development of AngIV-related pharmaceuticals as therapeutic agents in disorders where inhibition of the HGF/Met system would be clinically advantageous.

JPET Fast Forward. Published on November 30, 2011 as DOI: 10.1124/jpet.111.188136
This article has not been copyedited and formatted. The final version may differ from this version.

MATERIAL AND METHODS

Animals. C57BL/6 mice from Taconic farms were used in the lung colonization studies. Male Sprague-Dawley rats (250+ g) were obtained from Harlan Laboratories (CA, USA) for use in pharmacokinetic studies. Animals were housed and cared for in accordance with NIH guidelines as described in the "Guide for the Care and Use of Laboratory Animals".

Compounds. D-Nle-X-Ile-NH-$(CH_2)_5$-COOH; where X= various amino acids and Norleual (Nle-Tyr-Leu-ψ-$(CH_2$-$NH_2)^{3-4}$-His-Pro-Phe) were synthesized using Fmoc based solid phase methods in the Harding laboratory and purified by reverse phase HPLC. Purity and structure were verified by LC-MS. Hepatocyte growth factor (HGF) was purchased from R&D Systems (Minneapolis, MN).

Antibodies. Anti-Met was purchased from Cell Signaling Technology (Beverly, MA) and the phospho-Met antibody was purchased from AbCam, Inc (Cambridge,MA).

Cell culture. Human embryonic kidney cells 293 (HEK293) and Madin Darby canine kidney cells (MDCK) were grown in DMEM, 10% fetal bovine serum (FBS). Cells were grown to 100% confluency before use. HEK and MDCK cells were serum starved for 2-24 h prior to the initiation of drug treatment.

Blood Stability Studies. To compare the blood stability of Norleual and D-Nle-Tyr-Ile-NH-$(CH_2)_5$-$CONH_2$, a representative member of the 6-AH family, 20 µL of compound-containing vehicle (water [Norleual] or 30% ethanol [D-Nle-Tyr-Ile-NH-$(CH_2)_5$-$CONH_2$]) was added to 180 µL of heparinized blood and incubated at 37^{o}C for

JPET Fast Forward. Published on November 30, 2011 as DOI: 10.1124/jpet.111.188136
This article has not been copyedited and formatted. The final version may differ from this version.

various times. For Norleual, 37^{o}C incubations were stopped at 0, 20, 40, and 60 min, and for D-Nle-Tyr-Ile-NH-$(CH_2)_5$-$CONH_2$, incubations were stopped at 0, 1, 3 and 5 h.

At the end of each incubation, 20 µL of Nle^{1}- AngIV (100 µg/ mL) was added to each sample as an internal standard. D-Nle-Tyr-Ile-NH-$(CH_2)_5$-$CONH_2$ samples were centrifuged at 4^{o}C for 5 min at 2300x g to pellet erythrocytes, and the plasma was transferred to clean tubes. The Norleual and D-Nle-Tyr-Ile-NH-$(CH_2)_5$-$CONH_2$ samples were precipitated by adding 3 vol of ice-cold acetonitrile (ACN) and the samples were vortexed vigorously. All samples were centrifuged at 4^{o}C, 2300x g for 5 min and the supernatants were transferred to clean tubes. Samples were then evaporated to dryness in a Savant SpeedVac® concentrator (Thermo Fisher Scientific, Waltham, MA) , the residue was reconstituted in 225 µl 35% methanol, vortexed briefly, transferred to HPLC autosampler vials, and 100 µl injected into the HPLC system.

Samples were then separated by HPLC on an Econosphere C18 (100mm x 2.1mm) from Grace Davison Discovery Science (Deerfield, IL). Peaks were detected and analyzed by mass spectrographic methods using a LCMS-2010EV mass spectrometer (Shimadzu, Kyoto Japan). The mobile phase consisted of HPLC water (Sigma St. Louis, MO) with 0.1% trifluoroacetic or 0.1% heptafluorobutyric acid (Sigma St. Louis, MO) and varying concentrations of ACN or methanol. Separation was carried out using a gradient method, at ambient temperature and a flow rate of 0.3 mL/min (see below for more information). Stability half-lives were determined assuming a normal single phase exponential decay using Prism 5 graphical/statistical program (GraphPad, San Diego, CA).

JPET Fast Forward. Published on November 30, 2011 as DOI: 10.1124/jpet.111.188136
This article has not been copyedited and formatted. The final version may differ from this version.

IV Pharmacokinetics.

Surgerical Procedures. Male Sprague-Dawley rats (250+ g) were allowed food (Harlan Teklad rodent diet) and water *ad libitum* in our AAALAC certified animal facility. Rats were housed in temperature-controlled rooms with a 12 h light/dark cycle. The right jugular veins of the rats were catheterized with sterile polyurethane Hydrocoat™ catheters (Access Technologies, Skokie, IL, USA) under ketamine (Fort Dodge Animal Health, Fort Dodge, IA, USA) and isoflurane (Vet One™, MWI, Meridian, ID, USA) anesthesia. The catheters were exteriorized through the dorsal skin. The catheters were flushed with heparinized saline before and after blood sample collection and filled with heparin-glycerol locking solution (6 mL glycerol, 3 mL saline, 0.5 mL gentamycin (100mg/mL), 0.5 mL heparin (10,000 u/mL)) when not used for more than 8 h. The animals were allowed to recover from surgery for several days before use in any experiment, and were fasted overnight prior to the pharmacokinetic experiment.

Pharmacokinetic Study. Catheterized rats were placed in metabolic cages prior to the start of the study and time zero blood samples were collected. Animals were then dosed intravenously via the jugular vein catheters, with D-Nle-Tyr-Ile-NH-$(CH_2)_5$-$CONH_2$ (24mg/kg) in 30% ethanol. After dosing, blood samples were collected as follows (times and blood volumes collected are listed in chronological order):

Compound	**Time (min)**	**Blood Volume Collected (µl)**
D-Nle-Tyr-Ile-NH-$(CH_2)_5$-$CONH_2$	0, 12, 30, 60, 90, 120, 180, 240, 300	200, 200, 200, 200, 200, 300, 400, 500, 500

JPET Fast Forward. Published on November 30, 2011 as DOI: 10.1124/jpet.111.188136
This article has not been copyedited and formatted. The final version may differ from this version.

After each blood sample was taken, the catheter was flushed with saline solution and a volume of saline equal to the volume of blood taken was injected (to maintain total blood volume).

Blood Sample Preparation. Upon collection into polypropylene microfuge tubes without heparin, blood samples were immediately centrifuged at 4^{o}C, 2300x g for 5 min to remove any cells and clots and the serum transferred into clean microcentrifuge tubes. A volume of internal standard (Nle^{1}-AngIV, 100 µg/mL) equal to 0.1 times the sample serum volume was added. A volume of ice-cold acetonitrile equal to four times the sample serum volume was then added and the sample vortexed vigorously for 30 s. The supernatants were transferred to clean tubes, then held on ice until the end of the experiment, and stored at 4ºC afterward until further processing.

Serial dilutions of D-Nle-Tyr-Ile-NH-$(CH_2)_5$-$CONH_2$ in 30% ethanol were prepared from the stock used to dose the animals for standard curves. 20 µL of each serial dilution was added to 180 µL of blood on ice for final concentrations of 0.01µg/mL, 0.1µg/mL, 1µg/mL and 10µg/mL. The samples were centrifuged at 4^{o}C, 2300x g for 5 min and the serum transferred into polypropylene microcentrifuge tubes. A volume of internal standard (Nle^{1}-AngIV, 100µg/mL) equal to 0.1 times the sample serum volume was added. A volume of ice-cold acetonitrile equal to four times the sample serum volume was then added and the sample vortexed vigorously for 30 s. The supernatants were transferred to clean tubes and samples stored at 4ºC and processed alongside the pharmacokinetic study samples. All samples were evaporated to dryness in a Savant SpeedVac® concentrator. The residue was reconstituted in 225 µl 35% methanol and

vortexed briefly. The samples were then transferred to HPLC autosampler vials and 100 µl was injected into the HPLC system a total of 2 times (2 HPLC/MS analyses) for each sample.

Chromatographic System and Conditions. The HPLC/MS system used was from Shimadzu (Kyoto, Japan), consisting of a CBM-20A communications bus module, LC-20AD pumps, SIL-20AC auto sampler, SPD-M20A diode array detector and LCMS-2010EV mass spectrometer. Data collection and integration were achieved using Shimadzu LCMS solution software. The analytical column used was an Econosphere C18 (100mm x 2.1mm) from Grace Davison Discovery Science (Deerfield, IL, USA). The mobile phase consisted of HPLC grade methanol and water with 0.1% trifluoroacetic acid. Separation was carried out using a non-isocratic method (40% - 50% methanol over 10 min) at ambient temperature and a flow rate of 0.3 mL/min. For MS analysis, a positive ion mode (Scan) was used to monitor the m/z of D-Nle-Tyr-Ile-NH-$(CH_2)_5$-$CONH_2$ at 542 and the m/z of Nle^1-AngIV (used for internal standard) at 395. Good separation of D-Nle-Tyr-Ile-NH-$(CH_2)_5$-$CONH_2$ and the internal standard in blood was successfully achieved. No interfering peaks co-eluted with the analyte or internal standard. Peak purity analysis revealed a peak purity index for D-Nle-Tyr-Ile-NH-$(CH_2)_5$-$CONH_2$ of 0.95 and the internal standard of 0.94. D-Nle-Tyr-Ile-NH-$(CH_2)_5$-$CONH_2$ eluted at 5.06 min and the internal standard at 4.31 min. Data were normalized based on the recovery of the internal standard.

Pharmacokinetic Analysis. Pharmacokinetic analysis was performed using data from individual rats. The mean and standard deviation (SD) were calculated for the

JPET Fast Forward. Published on November 30, 2011 as DOI: 10.1124/jpet.111.188136
This article has not been copyedited and formatted. The final version may differ from this version.

group. Non-compartmental pharmacokinetic parameters were calculated from serum drug concentration-time profiles by use of WinNonlin® software (Pharsight, Mountain View, CA, USA). The following relevant parameters were determined where possible: area under the concentration-time curve from time zero to the last time point ($AUC_{0\text{-last}}$) or extrapolated to infinity ($AUC_{0\text{-}\infty}$), C_{max} concentration in plasma extrapolated to time zero (C_0), terminal elimination half-life ($t_{1/2}$), volume of distribution (Vd), and clearance (CL).

Microsomal Metabolism. Male rat liver microsomes were obtained from Celsis (Baltimore, MD, USA). The protocol from Celsis for assessing microsomal- dependent drug metabolism was followed with minor adaptations. An NADPH regenerating system (NRS) was prepared as follows: 1.7 mg/mL NADP, 7.8 mg/mL glucose-6-phosphate and 6 units/mL glucose-6-phosphate dehydrogenase were added to 10 mL 2% sodium bicarbonate and used immediately. 500 µM solutions of Norleual, D-Nle-Tyr-Ile-NH-$(CH_2)_5$-$CONH_2$, piroxicam, verapamil and 7-ethoxycoumarin (low, moderate and highly metabolized controls, respectively) were prepared in acetonitrile. Microsomes were suspended in 0.1M Tris buffer (pH 7.38) at 0.5 mg/mL and 100 µL of the microsomal suspension was added to pre-chilled microcentrifuge tubes on ice. To each sample, 640 µL 0.1M Tris buffer, 10 µL 500 µM test compound, and 250 µL of NRS was added. Samples were incubated in a rotisserie hybridization oven at 37ºC for the appropriate incubation times (10, 20, 30 40 or 60 min). 500 µL from each sample was transferred to tubes containing 500 µL ice-cold acetonitrile with internal standard per incubation sample. Standard curve samples were prepared in incubation buffer and 500 µL added to 500 µL ice-cold acetonitrile with internal standard. All samples were then analyzed by

JPET Fast Forward. Published on November 30, 2011 as DOI: 10.1124/jpet.111.188136
This article has not been copyedited and formatted. The final version may differ from this version.

high performance liquid chromatography/mass spectrometry. Drug concentrations were determined and loss of parent relative to negative control samples containing no microsomes was calculated. Clearance was determined by nonlinear regression analysis for k_e and $t_{1/2}$ and the equation $Cl_{int} = k_e$ Vd. *For* in vitro-in vivo correlation, Cl_{int} per kg body weight was calculated using the following measurements for Sprague-Dawley rats: 44.8 mg of protein per g of liver, 40 g of liver per kg of body weight.

HGF Binding. The binding of 6-AH analogs to HGF was assessed by competition using a soluble binding assay. 250µl of PBS containing human HGF (1.25ng) were incubated with ^{3}H-Hinge, the central dimerization domain of HGF, in the presence of varying concentrations of 6-AH analogs between 10^{-13} M to 10^{-7}M (half-log dilutions) for 40 min at 37^0C. The incubates were then spun through Bio-Gel P6 spin columns (400 µl packed volume) for 1 min to separate free and bound ^{3}H-Hinge and the eluent was collected. Five milliliters of scintillation fluid was added to the eluent, which contained the HGF bound ^{3}H-Hinge, and was then counted using scintillation counter. Total disintegrations per minute of bound ^{3}H-Hinge were calculated based on machine counting efficiency. The Ki values for the binding of the peptides were determined using the Prism 5. Competition binding curves were performed in triplicate. Preliminary kinetic studies indicated that equilibrium binding was reached by 40 min of incubation at 37^oC. ^{3}H- Hinge has recently been shown to bind to HGF with high affinity (Kawas et al., 2011).

HGF Dimerization. HGF dimerization was assessed using PAGE followed by silver staining (Kawas et al., 2011). Human HGF at a concentration of 0.08ng/µl with or

JPET Fast Forward. Published on November 30, 2011 as DOI: 10.1124/jpet.111.188136
This article has not been copyedited and formatted. The final version may differ from this version.

without 6-AH analogs was incubated with heparin at a final concentration of 5µg/ml. Loading buffer was then added to each sample and the mixture separated by native PAGE using gradient Criterion XT precast gels (4-12% Bis-Tris; Biorad Laboratories, Hercules, CA). Next the gel was silver stained for the detection of the HGF monomers and dimers. Bands were quantitated from digital images using a UVP phosphoimager (Upland, CA).

Western blotting. HEK293 cells were seeded in 6 well tissue culture plates and grown to 95% confluency in DMEM containing 10% FBS. The cells were serum deprived for 24 h prior to the treatment to reduce the basal levels of phospho-Met. Following serum starvation, cocktails comprised of vehicle and HGF with/without 6-AH analogs were prepared and pre-incubated for 30 min at room temperature. The cocktail was then added to the cells for 10 min to stimulate the Met receptor and downstream proteins. Cells were harvested using RIPA lysis buffer (Millipore; Billerica, MA) fortified with phosphatase inhibitor cocktails 1 and 2 (Sigma-Aldrich; St. Louis, MO). The lysate was clarified by centrifugation at 15,000 nx g for 15 min, protein concentrations were determined using the BCA total protein assay (Pierce), and then appropriate volumes of the lysates were diluted with 2x reducing Laemmli buffer and heated for ten min at 95° C. Samples containing identical amounts of protein were resolved using SDS-PAGE (Criterion, BioRad Laboratories), transferred to nitrocellulose, and blocked in Tris-buffered saline (TBS) containing 5% milk for 1 h at room temperature. The phospho-Met antibody were added to the blocking buffer at a final concentration of 1:1000 and incubated at 4° C overnight with gentle agitation. The membranes were then washed several times with water and TBS (PBS, 0.05% Tween-20), a 1:5000 dilution of

JPET Fast Forward. Published on November 30, 2011 as DOI: 10.1124/jpet.111.188136
This article has not been copyedited and formatted. The final version may differ from this version.

horseradish-peroxidase conjugated goat anti-rabbit antiserum was added, and the membranes further incubated for 1 h at room temperature. Proteins were visualized using the Supersignal West Pico Chemiluminescent Substrate system (Pierce, Fenton, MO) and molecular weights determined by comparison to protein ladders (BenchMark, Invitrogen, and Kaleidoscope, BioRad). Film images were digitized and analyzed using a UVP phosphoimager.

Cell proliferation. 5000 MDCK cells were seeded into the wells of a 96 well plates in 10% FBS DMEM. To induce cellular quiescence, the cells were serum deprived for 24 h prior to initiating the treatments. Following serum starvation, 10 ng/ml HGF alone and with various concentrations of 6-AH analogs or PBS vehicle were added to the media. The cells were allowed to grow under these conditions for 4 days with a daily addition of 6-AH analogs. On the fourth day, 1 mg/ml of 1-(4, 5-Dimethylthiazol-2-yl) 3, 5-diphenylformazan reagent (MTT, Sigma-Aldrich) prepared in PBS was added to the cells and incubated for 4 h. Dimethyl sulfoxide diluted in a .01M glycine buffer was added to solubilize the cell membranes and the absorbance of reduced MTT in the buffer was quantitated at 590 nm using a plate reader (Biotek Synergy 2, Winooski, VT). HGF-dependent proliferation was determined by subtracting the basal proliferation (in the absence of HGF) from total proliferation rates in groups containing HGF.

Scattering assay. MDCK cells were grown to 100% confluency on the coverslips in six-well plates and washed twice with PBS. The confluent coverslips were then aseptically transferred to new six well plates containing 900 µl serum free DMEM. Norleual, Hinge peptide, and/or HGF (20 ng/ml) were added to appropriate wells.

JPET Fast Forward. Published on November 30, 2011 as DOI: 10.1124/jpet.111.188136
This article has not been copyedited and formatted. The final version may differ from this version.

Control wells received PBS vehicle. Plates were incubated at 37°C with 5% CO_2 for 48 h. Media was removed and cells were fixed with methanol. Cells were stained with Diff-Quik Wright-Giemsa (Dade-Behring, Newark, DE) and digital images were taken. Coverslips were removed with forceps and more digital images were captured. Pixel quantification of images was achieved using Image J and statistics were performed using Prism 5 and InStat v.3.05 (GraphPad; San Diego, CA).

Lung colony formation. Six to eight month old C57BL/6 mice were injected with 400,000 B16-F10 cells in 200 µl PBS by tail vein injection and subsequently received daily intraperitoneal injections of either D-Nle-X-Cys-NH-$(CH_2)_5$-$CONH_2$ (10 µg/kg and 100µg/kg) or a PBS vehicle control. Two weeks later, mice were anesthetized and lungs were perfused with PBS and removed. Photos were taken and lungs were solubilized in 1% Triton x-100, 20 mM Tris, 0.15 M NaCl, 2 mM EDTA, and 0.02% sodium azide. Samples were disrupted by sonication (Mixonix, Farmingdale, NY) and spun. The supernatant was transferred to a 96 well plate and melanin absorbance at 410nm was measured using a plate reader.

Statistics. Independent one-way analysis of variance (ANOVA) (InStat v.3.05 and Prism 5) was used to determine differences among groups. Tukey-Kramar or Bonferroni's multiple comparison post-hoc tests were performed where necessary. Statistical comparisons of two groups were determined using the two-tailed Student's *t*-test (InStat v.3.05 and Prism 5).

JPET Fast Forward. Published on November 30, 2011 as DOI: 10.1124/jpet.111.188136
This article has not been copyedited and formatted. The final version may differ from this version.

RESULTS

The AngIV analog D-Nle-Tyr-Ile-NH-$(CH_2)_5$-$CONH_2$ is more metabolically stable than Norleual (Nle-Tyr-Leu-ψ-$(CH_2$-$NH_2)^{3-4}$-His-Pro-Phe): The AngIV-related peptidomimetic Norleual was previously shown to possess, anti-HGF/Met, anti-angiogenic, and anti-cancer activities (Yamamoto et al., 2010). The presence of unprotected peptide bonds at both the N- and C-terminal linkages predicts that Norleual should have poor metabolic stability and rapid clearance for the circulation, properties that may limit its clinical utility. In an attempt to overcome this limitation, a family of compounds, the 6-AH family was designed and synthesized to offer defense against exopeptidases. **Figure 1** demonstrates that as expected Norleual is unstable in heparinized blood while D-Nle-Tyr-Ile-NH-$(CH_2)_5$-$CONH_2$ exhibited improved stability.

The AngIV analog D-Nle-Tyr-Ile-NH-$(CH_2)_5$-$CONH_2$ has a much longer circulating half-life than Norleual (Nle-Tyr-Leu-ψ-$(CH_2$-$NH_2)^{3-4}$-His-Pro-Phe): As anticipated from the in-vitro blood stability data, D-Nle-Tyr-Ile-NH-$(CH_2)_5$-$CONH_2$ exhibited an extended in vivo elimination half-life of 1012 min after IV injection in rats. Other relevant pharmacokinetic parameters of D-Nle-Tyr-Ile-NH-$(CH_2)_5$-$CONH_2$ after a single IV bolus dose are summarized in **Table 1**. Serum data were modeled using WinNonlin® software to perform non-compartmental analysis. D-Nle-Tyr-Ile-NH-$(CH_2)_5$-$CONH_2$ appeared to be extensively distributed outside the central blood compartment and/or bound within the tissues as evidenced by its large volume of distribution (Vd). D-Nle-Tyr-Ile-NH-$(CH_2)_5$-$CONH_2$ is not expected to be highly bound to plasma proteins according to quantitative structure-activity relationship (QSAR) modeling (discussed below) and since total recovery from serum was greater than 35 %. These results,

JPET Fast Forward. Published on November 30, 2011 as DOI: 10.1124/jpet.111.188136
This article has not been copyedited and formatted. The final version may differ from this version.

which suggest that D-Nle-Tyr-Ile-NH-$(CH_2)_5$-$CONH_2$ is likely to be relatively hydrophobic, are in agreement with the outcome of QSAR modeling estimates generated by ADMET Predictor® that calculated an octanol:water partition coefficient of 28.18 for D-Nle-Tyr-Ile-NH-$(CH_2)_5$-$CONH_2$ (**Table 2**).

Not surprisingly because of its stability, hydrophobic character, and small size, D-Nle-Tyr-Ile-NH-$(CH_2)_5$-$CONH_2$ was predicted to be orally bioavailable. The P_{eff} value represents the predicted effective human jejunal permeability of the molecule. The predicted P_{eff} value for D-Nle-Tyr-Ile-NH-$(CH_2)_5$-$CONH_2$ (1.53) is intermediate between the predicted P_{eff} values for enalapril (1.25) and piroxicam (2.14), two orally bioavailable drugs. D-Nle-Tyr-Ile-NH-$(CH_2)_5$-$CONH_2$ was also predicted to be 42.68 percent unbound to plasma proteins in circulation, thus making it available for distribution into the tissues.

Also contributing to its slow removal from the blood was a lack of Phase I metabolism for D-Nle-Tyr-Ile-NH-$(CH_2)_5$-$CONH_2$. D-Nle-Tyr-Ile-NH-$(CH_2)_5$-$CONH_2$ exhibited no detectable metabolism over 90 min in an in-vitro metabolism assay using rat liver microsomes (data not shown). Together these data indicate that D-Nle-Tyr-Ile-NH-$(CH_2)_5$-$CONH_2$ is more metabolically stable than Norleual, possesses an elongated half-life in the circulation and penetrates tissue effectively. Overall these favorable pharmacokinetic properties justify the mechanistic and therapeutic evaluation of D-Nle-Tyr-Ile-NH-$(CH_2)_5$-$CONH_2$ and related molecules.

JPET Fast Forward. Published on November 30, 2011 as DOI: 10.1124/jpet.111.188136
This article has not been copyedited and formatted. The final version may differ from this version.

D-Nle-X-Ile-NH-$(CH_2)_5$-$CONH_2$ analogs bind HGF and compete with the ^{3}H-Hinge peptide for HGF binding:

Several members of the D-Nle-X-Ile-NH-$(CH_2)_5$-$CONH_2$, 6-AH family, were analyzed for the capacity to compete for ^{3}H-Hinge binding to HGF. As will be evident below, members of the 6-AH family display a varied ability to block the biological action of HGF. As such, the HGF binding properties of a selection of analogs with varying biological activity was assessed to determine if there was a relationship between inhibitory activity and affinity for HGF. The hypothesis that was put forth was that analogs are binding directly to HGF and affecting the sequestration of HGF in an inactive form. To begin the evaluation of this idea, we used a ^{3}H-Hinge peptide as a probe to assess direct HGF binding of the peptides. The use of ^{3}H-Hinge to probe the interaction was based on the ability of ^{3}H-Hinge to bind specifically and with high affinity to HGF (Kawas et al., 2011). A competition study was initiated with several derivatives of the D-Nle-X-Ile-NH-$(CH_2)_5$-$CONH_2$ family. This study demonstrated that different analogs have variable abilities to bind HGF, and that the analogs showing antagonism to HGF are acting as a Hinge mimics. D-Nle-X-Ile-NH-$(CH_2)_5$-$CONH_2$ derivatives were found to compete with Hinge for HGF binding and exhibited a range of affinities for HGF, with K_is ranging from $1.37x10^{-7}$- $1.33x10^{-10}$M (**Figure 2**). As expected it appears to be relationship between a compound's ability to bind HGF and its capacity to block dimerization and inhibit HGF-dependent activities (see **Figures 4, 5, 6**).

D-Nle-X-Ile-NH-$(CH_2)_5$-$CONH_2$ analogs block HGF Dimerization: Several reports have shown that HGF needs to form homodimers and/or multimers, prior to its activation of Met (Chirgadze et al., 1999; Gherardi et al., 2006). This dimer is arranged

JPET Fast Forward. Published on November 30, 2011 as DOI: 10.1124/jpet.111.188136
This article has not been copyedited and formatted. The final version may differ from this version.

in a head to tail orientation; the dimer interface comprises a central region, the hinge region that is important for the proper dimer formation and orientation. A homologous sequence-conservation screen against all possible transcripts that were independent of and not derived from angiotensinogen looking for similarities to AngIV identified partial homology with the hinge region (Yamamoto et al., 2010) of the plasminogen family of proteins, which include plasminogen itself, its anti-angiogenic degradation product, angiostatin, and the protein hormones heptocyte growth factor (HGF) and macrophage stimulating protein (MSP). Moreover, the AngIV analog Norleual, which is a potent inhibitor of the HGF/Met system, was shown to bind to HGF and block its dimerization (Kawas et al., 2011). This knowledge coupled with the demonstration that some members of the 6-AH family bound with high affinity to the hinge region of HGF led to the expectation that other active AngIV analogs, like 6-AH family members, could be expected to inhibit HGF dimerization and that the ability of an individual analog to bind HGF and inhibit HGF-dependent processes should be reflected in its capacity to attenuate dimerization. The data in **Figure 3** confirm this expectation by demonstrating that D-Nle-Cys-Ile-NH-$(CH_2)_5$-$CONH_2$ and D-Nle-Tyr-Ile-NH-$(CH_2)_5$-$CONH_2$, which bind HGF with high affinity (**Figure 2**) and effectively attenuate HGF-dependent processes (**Figures 4, 5, 6**) completely block HGF dimer formation. Conversely D-Nle-Met-Ile-NH-$(CH_2)_5$-$CONH_2$, which has low affinity for HGF (**Figure 2**) and exhibits little anti-HGF/Met activity, is unable to block dimerization at the concentration tested. The D-Nle-Trp-Ile-NH-$(CH_2)_5$-$CONH_2$ analog, which exhibits intermediate inhibition of dimerization, predictably has a moderate affinity for HGF and a moderate ability to inhibit HGF-dependent processes (**Figures 4, 5, 6**). Together these data confirm the expectation

JPET Fast Forward. Published on November 30, 2011 as DOI: 10.1124/jpet.111.188136
This article has not been copyedited and formatted. The final version may differ from this version.

that active 6-AH analogs can block dimerization and further that dimerization inhibitory potential of an analog translates, at least qualitatively, to its capacity to block HGF-dependent processes.

D-Nle-X-Ile-NH-$(CH_2)_5$-$CONH_2$ analogs attenuates HGF-dependent Met signaling:

After establishing that the 6-AH family members exhibit a range of HGF binding and dimerization inhibitory profiles, we next determined whether these properties would parallel a compound's ability to inhibit Met signaling. Characteristic of tyrosine kinase-linked growth factor receptors like Met is a requisite tyrosine residue auto-phosphorylation step, which is essential for the eventual recruitment of various SH2 domain signaling proteins. Thus we evaluated the ability of several 6-AH analogs to induce Met tyrosine phosphorylation. As anticipated, the data in **Figure 4** demonstrate that both D-Nle-Cys-Ile-NH-$(CH_2)_5$-$CONH_2$ and D-Nle-Tyr-Ile-NH-$(CH_2)_5$-$CONH_2$, which bind HGF with high affinity (**Figure 2**) and effectively block its dimerization (**Figure 3**) were able to block Met auto-phosphorylation. The D-Nle-Trp-Ile-NH-$(CH_2)_5$-$CONH_2$ analog had intermediate inhibitory activity, and the D-Nle-Met-Ile-NH-$(CH_2)_5$-$CONH_2$ analog showed no ability to effect on Met activation. Together, these data indicate that the capacity of 6-AH analogs to inhibit HGF-dependent Met activation paralleled their HGF binding affinity and their capacity to block dimerization.

D-Nle-X-Ile-NH-$(CH_2)_5$-$CONH_2$ analogs affect HGF/Met stimulated MDCK cell proliferation:

Met activation initiates multiple cellular responses including increased proliferation and motility, enhanced survival, and differentiation (Zhang and Vande Woude, 2003). As an

JPET Fast Forward. Published on November 30, 2011 as DOI: 10.1124/jpet.111.188136
This article has not been copyedited and formatted. The final version may differ from this version.

initial test of the ability of 6-AH family members to alter HGF-dependent cellular activity we evaluated the capacity of several members of the family to modify the proliferative activity of Madin-Darby canine kidney (MDCK) cells, a standard cellular model for investigating the HGF/Met system (Stella and Comoglio, 1999). As seen in **Figure 5** there is a wide range of inhibitory activity against HGF dependent cellular proliferation. Similar to the results from the binding and dimerization experiments the Cys^2 and Tyr^2 analogs exhibited marked inhibitory activity. The Asp^2 analog, which had not been evaluated in the earlier studies, also exhibited pronounced inhibitory activity. The Trp^2, Phe^2, and Ser^2 analogs all showed inhibitory activity, albeit less than that observed with the most potent analogs. The decrease in HGF-dependent MDCK proliferation below control levels for some compounds is not surprising since the experiment was carried in 2% serum, which likely contains some level of HGF. The Hinge peptide (KDYIRN), which represents the dimerization domain of HGF, was included as a positive control. A recent study has demonstrated that Hinge binds to HGF with high affinity blocking its dimerization and acting as a potent inhibitor of HGF-dependent cellular activities including MDCK proliferation (Kawas et al., 2011).

D-Nle-X-Ile-NH-$(CH_2)_5$-$CONH_2$ analogs modify HGF/Met mediated cell scattering in MDCK cells:

Cell scattering is the hallmark effect of HGF/Met signaling; a process characterized by decreased cell adhesion, increased motility, and increased proliferation. The treatment of MDCK cells with HGF initiates a scattering response that occurs in two stages. First, the cells lose their cell-to-cell adhesion and become polarized. Second, they separate completely and migrate away from each other. It is expected that if the 6-AH family

JPET Fast Forward. Published on November 30, 2011 as DOI: 10.1124/jpet.111.188136
This article has not been copyedited and formatted. The final version may differ from this version.

members are capable of inhibiting the HGF/Met system then they should be able to modify HGF dependent MDCK cell scattering.

Figures 6 A & B indicate that those analogs that were previously found to block HGF dimerization were effective inhibitor of HGF/Met mediated cell scattering in MDCK cells, while those analogs with poor affinity for HGF were ineffective. **Figure 7** shows a correlation between the blockade of HGF dimerization and HGF binding affinity and the ability to prevent MDCK cell scattering.

D-Nle-Cys-Ile-NH-$(CH_2)_5$-$CONH_2$ inhibits B16-F10 murine melanoma cell migration and lung colony formation:

To evaluate the prospective utility of the 6-AH family members' as potential therapeutics, we examined the capacity of [D-Nle-Cys-Ile-NH-$(CH_2)_5$-$CONH_2$], an analog that exhibits a strong inhibitory profile against HGF-dependent Met activation, to suppress the migratory and lung colony-forming capacity of B16-F10 murine melanoma cells. B16 melanoma cells over-express Met (Ferraro et al., 2006), and were chosen for these studies because Met signaling is critical for their migration, invasion, and metastasis. As a final test for the physiological significance of the 6-AH family blockade of Met-dependent cellular outcomes, we evaluated the ability of D-Nle-Cys-Ile-NH-$(CH_2)_5$-$CONH_2$ to inhibit the formation of pulmonary colonies by B16-F10 cells after tail vein injection in mice. **Figure 8a** illustrates the inhibitory response that was observed with daily intraperitoneal injections at two doses (10µg/kg/day and 100µg/kg/day) of [D-Nle-Cys-Ile-NH-$(CH_2)_5$-$CONH_2$]. **Figure 8b** provides a quantitative assessment of pulmonary colonization by measuring melanin content, which reflects the level of melanoma colonization. Together these data demonstrate that treatment of melanoma

JPET Fast Forward. Published on November 30, 2011 as DOI: 10.1124/jpet.111.188136
This article has not been copyedited and formatted. The final version may differ from this version.

cells with D-Nle-Cys-Ile-NH-$(CH_2)_5$-$CONH_2$ radically prevented lung colonization and highlight the potential utility of the use of 6-AH analogs as potential anti-cancer agents.

JPET Fast Forward. Published on November 30, 2011 as DOI: 10.1124/jpet.111.188136
This article has not been copyedited and formatted. The final version may differ from this version.

DISCUSSION:

Recently interest has grown in developing therapeutics targeting the HGF/Met system. At present this interest has been primarily driven by the realization that over-activation of the HGF/c-Met system is a common characteristic of many human cancers (Comoglio et al., 2008; Eder et al., 2009). The potential utility of anti-HGF/Met drugs, however, goes well beyond their use as anti-cancer agents. For example, the recognized involvement of the HGF/c-Met system in the regulation of angiogenesis (see review-You and McDonald, 2008) supports the potential utility of HGF/Met antagonists for the treatment of disorders in which control of tissue vascularization would be clinically beneficial. These could include hyper-vascular diseases of the eye like diabetic retinopathy and the wet type of macular degeneration. In both cases anti-angiogenic therapies are currently in use (see reviews- Barkmeier and Carvounis 2011; Jeganathan, 2011). Anti-angiogenics are also being examined as treatment options in a variety of other disorders ranging from obesity where adipose tissue vascularization is targeted (Daquinag et al., 2011), to chronic liver disease (Coulon et al., 2011), to psoriasis where topical application of anti-angiogenic drugs is being considered (Canavese et al., 2010).

Currently the pharmaceutical industry is employing two general approaches to block Met-dependent cellular activities (Eder et al., 2009; Liu X et al 2010). The first involves the development of single-arm humanized antibodies to HGF (Burgess et al., 2006; Stabile et al., 2008) or Met (Martens et al., 2006). The second approach utilizes “kinase inhibitors”, which block the intracellular consequences of Met activation. These ‘kinase inhibitors” are small hydrophobic molecules that work intracellularly to compete

for the binding of ATP to the kinase domain of Met thus inhibiting receptor autophosphorylation (Morotti et al., 2002; Christensen et al., 2003; Sattler et al., 2003). Despite the promise of the biologic and kinase-inhibitor approaches, which are currently represented in clinical trials, both have limitations arising from toxicity or specificity considerations and/or cost (Hansel et al., 2010; Maya, 2010).

A third approach, which our laboratory has been pursuing exploits a step in the activation process of the HGF-Met system; namely the need for HGF to pre-dimerize before it is able to activate Met. Thus we have targeted the dimerization process by developing molecules that mimic the dimerization domain, the hinge region, with idea that they can act as dominant negative replacements. Recent studies have validated this general approach demonstrating that molecules designed around angiotensin IV (Yamamoto et al, 2010) or the hinge sequence itself (Kawas et al., 2011) can bind HGF, block its dimerization, and attenuate HGF-dependent cellular actions. The studies described herein represent a first step toward producing useful therapeutics targeted at HGF dimerization. The primary focus of this study was to improve the pharmacokinetic characteristics of a parent compound, Norleual (Yamamoto et al., 2010) while maintaining biological activity. To this end we successfully synthesized and evaluated a family of new molecules, the 6-AH family [D-Nle-X-Ile-NH-$(CH_2)_5$-COOH]. A subset of these molecules not only had improved metabolic stability and circulating $t_{1/2}$ but exhibited excellent in vitro and in vivo activity.

In addition to characterizing a new family of HGF/Met antagonists, the present investigation demonstrated a qualitative relationship between the ability of a compound to bind HGF and block HGF dimerization and its observed in vitro biological activity.

Moreover these studies provide initial structure-activity data and pave the way for more extensive evaluation. The chemical modifications that were made at the N- and C-terminals of the AngIV molecule and the resultant improvement in metabolic stability highlight the critical role played by exopeptidases in the metabolism of AngIV-derived molecules. The demonstrated importance of protecting the terminals to pharmacokinetic characteristics suggests numerous additional synthetic approaches that may be applicable including the insertion of non-peptide linkages (see Sardinia et al., 1994) between the first and second amino acids, the replacement of the N-terminal amino acid with a non-α amino acid, and N-terminal acylation.

In sum these studies further validate the notion that targeting the dimerization domain of HGF is an effective means of inhibiting the HGF/Met system. Further they demonstrate that molecules with favorable pharmacokinetic characteristics can be produced thus highlighting their potential clinical utility.

JPET Fast Forward. Published on November 30, 2011 as DOI: 10.1124/jpet.111.188136
This article has not been copyedited and formatted. The final version may differ from this version.

AUTHORSHIP CONTRIBUTIONS

Participated in research design: Harding, Kawas, Yamamoto, Wright, McCoy

Conducted experiments: Kawas, McCoy, Yamamoto

Preformed Data analysis: Kawas, McCoy, Yamamoto, Harding

Wrote or contributed to the writing of the manuscript: Kawas, McCoy, Harding, Wright

REFERENCES

Barkmeier A. J & Carvounis P E (2011) Retinal pigment epithelial tears and the management of exudative age-related macular degeneration. *Seminars in Ophthalmology* 26: 94-103.

Birchmeier C, Birchmeier W, Gherardi E, and Vande Woude GF (2003) Met, metastasis, motility and more. *Nature Reviews: Molecular Cell Biology* 4: 915-925.

Borowiak M, Garratt AN, Wüstefeld T, Strehle M, Trautwein C and Birchmeier C (2004) Met provides essential signals for liver regeneration. *Proceedings of the National Academy of Sciences* 101: 10608-10613.

Burgess T, Coxon A, Meyer S, Sun J, Rex K, Tsuruda T, Chen Q, Ho SY, Li L, Kaufman S, McDorman K, Cattley RC, Elliott G, Zhang K, Feng X, Jia XC, Green L, Radinsky R and Kendall R (2006) Fully human monoclonal antibodies to hepatocyte growth factor with therapeutic potential against hepatocyte growth factor/c-Met-dependent human tumors. *Cancer Research* 66:1721-1729.

Canavese M, Altruda F, Ruzicka T, and Schauber J (2010) Vascular endothelial growth factor (VEGF) in the pathogenesis of psoriasis-A possible target for novel therapies? *Journal of Dermatological Science* 58: 171-176.

Chirgadze DY, Hepple JP, Zhou H, Byrd RA, Blundell TL and Gherardi E (1999) Crystal structure of the NK1 fragment of HGF/SF suggests a novel mode for growth factor dimerization and receptor binding. *Nature Structural Biology* 6: 72-79.

Christensen JG Burrows J and Salgia R (2005) c-Met as a target for human cancer and characterization of inhibitors for therapeutic intervention. *Cancer Letters* 225:1-26.

Christensen JG, Schreck R, Burrows J, Kuruganti P, Chan E, Le P, Chen J, Wang X, Ruslim L, Blake R, Lipson KE, Ramphal J, Do S, Cui JJ, Cherrington JM and Mendel DB (2003) A selective small molecule inhibitor of c-Met kinase inhibits c-Met-dependent phenotypes in vitro and exhibits cytoreductive antitumor activity in vivo. *Cancer Research* 63:7345-7355.

Comoglio PM, Giordano S and Trusolino L (2008) Drug development of MET inhibitors: targeting oncogene addiction and expedience. *Nature Reviews: Drug discovery* 7:504-516.

Coulon S, Heindryckx F, Geerts A, Van Steenkiste, C Colle I, and Van Vlierberghe H (2011) Angiogenesis in chronic liver disease and its complications. *Liver International* 31: 146-162.

Daquinag A C, Zhang Y, and Kolonin M G (2011) Vascular targeting of adipose tissue as an anti-obesity approach. *Trends in Pharmacological Sciences* 32:300-307.

Donate LE, Gherardi E, Srinivasan N, Sowdhamini R, Aparicio S and Blundell TL (1994) Molecular evolution and domain structure of plasminogen-related growth factors (HGF/SF and HGF1/MSP). *Protein Science* 3:2378-2394.

Eder JP, Vande Woude GF, Boerner SA and LoRusso PM (2009) Novel therapeutic inhibitors of the c-Met signaling pathway in cancer. *Clinical Cancer Research* 15:2207-2214.

Ferraro D, Corso S, Fasano E, Panieri E, Santangelo R, Borrello S, Giordano S, Pani G and Galeotti T (2006) Pro-metastatic signaling by Met through RAC-1 and reactive oxygen species (ROS). *Oncogene* 25:3689-3698.

Gherardi E, Sandin S, Petoukhov MV, Finch J, Youles ME, ofverstedt L-Gr, Miguel RN, Biundell TL, Vande Woude GF, Skoglund U and Svergun DI (2006) Structural basis of hepatocyte growth factor/scatter factor and MET signalling, *Proceedings of the National Academy of Sciences* 103:4046-4051.

Halaban R, Rubin JS, Funasaka Y, Cobb M, Boulton T, Faletto D, Rosen E, Chan A, Yoko K, White W and et al. (1992) Met and hepatocyte growth factor/scatter factor signal transduction in normal melanocytes and melanoma cells. *Oncogene* 7:2195-2206.

Hansel TT, Kropshofer H, Singer T, Mitchell JA and George AJ (2010) The safety and side effects of monoclonal antibodies. *Nature Reviews*. *Drug Discovery* 9:325-338.

Jeganathan, V. S. E. (2011) Anti-angiogenesis drugs in diabetic retinopathy. *Current Pharmaceutical Biotechnology* 12:369-372.

Kakazu A, Chandrasekher G, and Bazan HE (2004) HGF protects corneal epithelial cells from apoptosis by the PI-3K/Akt-1/Bad- but not the ERK1/2-mediated signaling pathway. *Investigative Ophthalmology and Visual Science* 45:3485-3492.

Kanda S, Kanetake H and Miyata Y (2006) HGF-induced capillary morphogenesis of endothelial cells is regulated by Src. *Biochemical & Biophysical Research Communications* 344:617-622.

Kawas LH, Yamamoto BJ, Wright JW, and Harding JW (2011) Mimics of the dimerization domain of hepatocyte growth factor exhibit anti-met and anti-cancer activity. *Journal of Pharmacology and Experimental Therapeutics* 339: 509-518.

Liu X, Newton RC and Scherle PA (2010) Developing Met pathway inhibitors for cancer therapy: progress and challenges. *Trends in Molecular Medicine* 16:37-45.

Liu X, Yao W, Newton RC. and Scherle PA (2008) Targeting the Met signaling pathway for cancer therapy. *Expert Opinion on Investigational Drugs* 17:997-1011.

Lokker NA, Mark MR, Luis EA, Bennett GL, Robbins KA, Baker JB, and Godowski PJ (1992) Structure-function analysis of hepatocyte growth factor: identification of variants that lack mitogenic activity yet retains high affinity receptor binding. The *EMBO Journal* 11:2503-2510.

Martens T, Schmidt N-O, Eckerich C, Fillbrandt R, Merchant M, Schwall R, Westphal M and Lamszus K (2006) A novel one-armed anti-c-Met antibody inhibits glioblastoma growth In vivo. *Clinical Cancer Research* 12:6144.

Maya BL (2010) Endocrine side effects of broad-acting kinase inhibitors. *Endocrine-Related Cancer* 17:233-244.

Morotti A, Mila S, Accornero P, Tagliabue E, and Ponzetto C (2002) K252a inhibits the oncogenic properties of Met, the HGF receptor. *Oncogene* 21:4885-4893.

Ratajczak MZ, Marlicz W, Ratajczak J, Wasik M, Machalinski B, Carter A and Gewirtz AM (1997) Effect of hepatocyte growth factor on early human haemopoietic cell development. *British Journal of Haematology* 99:228-236.

Sardinia, MF, Hanesworth, JM, Krishnan, R, and Harding, JW (1994) AT4 receptor structure-binding relationship: N-terminal-modified angiotensin IV analogues. *Peptides 15*:1399-1406.

Sattler M, Pride YB, Ma P, Gramlich JL, Chu SC, Quinnan LA, Shirazian S, Liang C, Podar K, Christensen JG, and Salgia R (2003) A novel small molecule met inhibitor induces apoptosis in cells transformed by the oncogenic TPR-MET tyrosine kinase. *Cancer Research* 63:5462-5469.

Sheth PR, Hays JL, Elferink LA, and Watowich SJ (2008) Biochemical basis for the functional switch that regulates hepatocyte growth factor receptor tyrosine kinase activation *Biochemistry* 47:4028-4038.

Stabile LP, Rothstein ME, Keohavong P, Jin J, Yin J, Land SR, Dacic S, Luong TM, Kim KJ, Dulak AM and Siegfried JM (2008) Therapeutic targeting of human hepatocyte growth factor with a single neutralizing monoclonal antibody reduces lung tumorigenesis. *Molecular Cancer Therapeutics* 7:1913-1922.

Stella MC and Comoglio PM (1999) HGF: a multifunctional growth factor controlling cell scattering. *International Journal of Biochemistry & Cell Biology* 31:1357-1362.

Thompson J, Dolcet X, Hilton M, Tolcos M and Davies AM (2004) HGF promotes survival and growth of maturing sympathetic neurons by PI-3 kinase- and MAP kinase-dependent mechanisms. *Molecular and Cellular Neurosciences* 27:441-452.

Wright JW, Stubley L, Pederson ES, Kramar EA, Hanesworth JM and Harding JW (1999) Contributions of the brain angiotensin IV-AT4 receptor subtype system to spatial learning. *J Neuroscience* 19:3952-3961.

You WK, McDonald DM (2008) The hepatocyte growth factor/c-Met signaling pathway as a therapeutic target to inhibit angiogenesis. *BMB Rep.* 41:833-839.

Yamamoto BJ, Elias PD, Masino JA, Hudson BD, McCoy AT, Anderson ZJ, Varnum MD, Sardinia MF, Wright JW and Harding JW (2010) The angiotensin IV analog Nle-Tyr-Leu-Ψ-CH_2-NH_2)$^{3-4}$-His-Pro-Phe (Norleual) can act as a hepatocyte growth factor/Met inhibitor. *Journal of Pharmacology and Experimental Therapeutics* 333:161-173.

You WK and McDonald DM (2008). The hepatocyte growth factor/c-Met signaling pathway as a therapeutic target to inhibit angiogenesis. *BMB Reports* 41:833-839.

Youles M, Holmes O, Petoukhov MV, Nessen MA, Stivala S, Svergun DI, and Gherardi E (2008) Engineering the NK1 fragment of hepatocyte growth factor/scatter factor as a MET receptor antagonist. *Journal of Molecular Biology* 377:616-622.

Zhang YW and Vande Woude GF (2003) HGF/SF-met signaling in the control of branching morphogenesis and invasion. *Journal of Cellular Biochemistry* 88:408-417.

FOOTNOTES

a) Leen Kawas and Alene McCoy contributed equally to the generation and presentation of the data described in this study.

b) This work was supported by a grant from the Adler Foundation to JWH.

c) JWW and JWH are founders and shareholders in M^3 Biotechnology, LLC, which is developing pharmaceuticals based on this technology.

d) An abstract of this work [Kawas LH, Yamamoto BJ, Wright JW, Harding JW. Development of Angiotensin IV Analogs as Hepatocyte Growth Factor/Met Antagonists and Anti-Cancer Agents.] was presented previously at the 2011 FASEB meetings.

JPET Fast Forward. Published on November 30, 2011 as DOI: 10.1124/jpet.111.188136
This article has not been copyedited and formatted. The final version may differ from this version.

LEGENDS FOR FIGURES

Fig.1 Stability of Norleual in rat blood as compared to D-Nle-Tyr-Ile-NH-$(CH_2)_5$-$CONH_2$.

Norleual and D-Nle-Tyr-Ile-NH-$(CH_2)_5$-$CONH_2$ were incubated in heparinized rat blood at 37ºC; the figure shows percent recovery over time (mean ± SD). The calculated stability $t_{1/2}$ based on single phase exponential decay for Norleual was 4.6 min and for D-Nle-Tyr-Ile-NH-$(CH_2)_5$-$CONH_2$ stability $t_{1/2}$ was 79.97 min.

Fig.2. Binding of D-Nle-X-Ile-NH-$(CH_2)_5$-$CONH_2$ analogs to HGF. Representative curves illustrating the competition of D-Nle-X-Ile-NH-$(CH_2)_5$-$CONH_2$ analogs for ^{3}H-Hinge binding to HGF. The D-Nle-X-Ile-NH-$(CH_2)_5$-$CONH_2$ analogs and ^{3}H-Hinge ($13.3x10^{-12}$M) were incubated with 1.25ng of HGF for 40 min at 37^{o}C in 0.25 ml of buffer. HGF-bound Hinge was eluted from Bio-Gel P6 columns after the addition of different concentrations of the D-Nle-X-Ile-NH-$(CH_2)_5$-$CONH_2$ analogs (10^{-13}-10^{-7}M). The radioactivity of the eluted solutions was quantitated using scintillation counting. These data demonstrate that the D-Nle-X-Ile-NH-$(CH_2)_5$-$CONH_2$ analogs exhibit a range of affinities for HGF. The K_is for the Met, Trp, Cys , and Tyr analogs were respectively determined to be: $1.375x10^{-07}$M , $3.372x10^{-09}$M, $1.330x10^{-10}$M, and $2.426x10^{-10}$M; N=9. D-Nle-Cys-Ile-NH-$(CH_2)_5$-$CONH_2$, D-Nle-Met-Ile-NH-$(CH_2)_5$-$CONH_2$, D-Nle-Trp-Ile-NH-$(CH_2)_5$- $CONH_2$, D-Nle-Tyr-Ile-NH-$(CH_2)_5$- $CONH_2$.

Figure 3. Inhibition of HGF dimerization by D-Nle-X-Ile-NH-$(CH_2)_5$-$CONH_2$ analogs. HGF spontaneously dimerizes when incubated in PBS in the presence of heparin. HGF was incubated without (control) or with various drug candidates at 10^{-10}M. These include

JPET Fast Forward. Published on November 30, 2011 as DOI: 10.1124/jpet.111.188136
This article has not been copyedited and formatted. The final version may differ from this version.

the derivatives of D-Nle-X-Ile- (6) amino-hexanoic amide, an AngIV-based analog family, where X= Tyr, Cys, Trp, and Met. After 30 minute incubation, samples were cross-linked with BS3, separated by gel electrophoresis, and silver stained. Band density was quantified and used to determine the level of HGF dimerization in each group. Treatment groups (Tyr, Cys, Trp) were statistically different than the HGF treated group ($P<0.05$; N=8) (**A**) Representative gel. (**B**) Pooled and quantified data.

Figure 4. Inhibition of Met phosphorylation by D-Nle-X-Ile-NH-$(CH_2)_5$-$CONH_2$ analogs. HEK293 cells were treated for 10 min with HGF+/- Nle-X-Ile-(6) amino-hexanoic amide analogs at the indicated concentrations. HEK293 cell lysates were immunoblotted with anti-phospho-Met and anti-Met antibodies. The differences in the mean values for Met phosphorylation among the indicated treatment groups (Nle-X-Ile-(6) amino-hexanoic amide analogs) compared to the HGF treated group were greater than would be expected by chance ($P <0.05$; N=6). The Met group was not different than the HGF group ($P>0.05$; N=6).

Figure 5. Effects of D-Nle-X-Ile-NH-$(CH_2)_5$-$CONH_2$ analogs on MDCK cell proliferation. MDCK cells were treated with a PBS vehicle (negative control), HGF, or HGF in combination with Nle-X-Ile-(6)-amino-hexanoic amide analogs (X= L-amino acid) at 10^{-10}M concentration. The Hinge peptide (KDYIRN), which represents the dimerization domain of HGF, was included as a positive control. The cells were allowed to grow for 4 days. Cell numbers were estimated on the fourth day with an MTT assay by measuring absorbance at 590. % HGF-dependent proliferation: control values were

JPET Fast Forward. Published on November 30, 2011 as DOI: 10.1124/jpet.111.188136
This article has not been copyedited and formatted. The final version may differ from this version.

subtracted from all values to determine HGF-induced increase in cell proliferation. N=6. *** p<0.001. ** p<0.001, * p<0.05, ns: not significant.

Figure 6. Effect of D-Nle-X-Ile-NH-$(CH_2)_5$-$CONH_2$ analogs on HGF-dependent scattering in MDCK cells. Cell scattering in which cells lose the cell-to-cell contacts and then migrate rapidly is the classic response to HGF. MDCK cells, the gold standard cellular model for studying the HGF/Met system, were grown to 100% confluence on cover slips and then placed in a clean plate. The cells were stimulated to scatter off of the cover slip by adding 20 ng/ml of HGF to the media alone or in combination with Nle-X-Ile-(6) amino-hexanoic amide analogs (X= L-amino acid). After 48 h of scattering, the cells were fixed with methanol and stained with Diff-Quik. The coverslips were removed to reveal the ring of cells that had scattered off of the cover slip and onto the plate. (**A**) The effect of HGF on scattering was quantitated by determining by densitometry of the digital images from scattered cells. ANOVA analysis indicates that the Tyr + HGF, Cys + HGF, and Trp + HGF treated groups were different from the HGF alone group but not different from the control group. The HGF and HGF + Met groups were not different. N=8, p<0.05 (**B**) Representative pictures of MDCK cells scattering off the coverslips.

Figure 7: Correlation between inhibition of MDCK cell scattering and interference with dimerization and the affinity to bind HGF. Three derivatives of the D-Nle-X-Ile-(6)amino-hexanoic amide, where X is: Cys, Trp, or Met were examined to determine whether the percent of inhibition of dimerization and the binding affinity for each compound for HGF could be correlated to in vitro cellular activity, namely inhibition of MDCK cell scattering. The figure shows a strong correlation between percent inhibition

JPET Fast Forward. Published on November 30, 2011 as DOI: 10.1124/jpet.111.188136
This article has not been copyedited and formatted. The final version may differ from this version.

of HGF dimerization (◆; R^2=0.9809) and for binding affinity to HGF (●; K_i Values; R^2=0.9903) and percent inhibition of HGF-dependent cell scattering

Figure 8. Inhibition of B16-F10 melanoma lung colonization by D-Nle-Cys-Ile-NH-$(CH_2)_5$-$CONH_2$. 400,000 B16-F10 murine melanoma cells were injected into the tail vein of C57BL/6 mice. Mice received daily IP injections of D-Nle-Cys-Ile-(6)-amino-hexanoic amide (10µg/kg/day or 100µg/kg/day) or PBS vehicle.(**A**) After 14 days, the lungs from D-Nle-Cys-Ile-(6)-amino-hexanoic amide treated mice exhibited an obvious reduction in melanoma colonies when compared to untreated controls. (**B**) After removal, lungs were homogenized and total melanin content was determined spectrophotometrically and used to quantify total pulmonary melanoma colonization in vehicle treated and D-Nle-Cys-Ile-(6)-amino-hexanoic amide treated. Ungrafted age-matched control lungs exhibited a background absorbance at 410nm. N=15, Mean ± SEM; * P<0.05, *** P<0.001.

JPET Fast Forward. Published on November 30, 2011 as DOI: 10.1124/jpet.111.188136
This article has not been copyedited and formatted. The final version may differ from this version.

Table.1. WinNonlin® estimated pharmacokinetic parameters for D-Nle-Tyr-Ile-NH-$(CH_2)_5$-$CONH_2$ after intravenous administration in adult male Sprague-Dawley rats

Mean+/- SEM; n = 5. $AUC_{0-\infty}$ = area under the curve. Vd= volume of distribution. Cp^0= initial concentration of drug in serum. $t_{1/2}$= biological half-life. KE= rate of elimination. CL= clearance rate.

Pharmacokinetic Parameter	D-Nle-Tyr-Ile-NH-$(CH_2)_5$-$CONH_2$ (Mean ± SEM)
AUC0-∞ (min.ng/mL)	692.5 ± 293.2
Vd (L/kg)	104186.8 ± 65034.3
Cp^0 (ng/mL)	68.2 ± 32.2
t1/2 (min)	1012.0 ± 391.4
KE (min-1)	0.001 ± 0.0002
CL (L/min/kg)	58.3 ± 15.6

JPET Fast Forward. Published on November 30, 2011 as DOI: 10.1124/jpet.111.188136
This article has not been copyedited and formatted. The final version may differ from this version.

Table 2. Predicted physiochemical properties of D-Nle-Tyr-Ile-NH-$(CH_2)_5$-$CONH_2$.

The physiochemical properties of D-Nle-Tyr-Ile-NH-$(CH_2)_5$-$CONH_2$ were estimated following modeling with ADMET Predictor® software. LogP is the octanol:water partitioning coefficient. P_{eff} is the predicted effective human jejunal permeability. P_{avg} is the approximate average intestinal permeability along the entire human intestinal tract. Pr_{Unbnd} is the percent unbound to plasma proteins.

Physicochemical Property	Predicted Value
logP	1.45
P_{eff}	1.53
P_{avg}	0.39
Pr_{Unbnd}	42.68

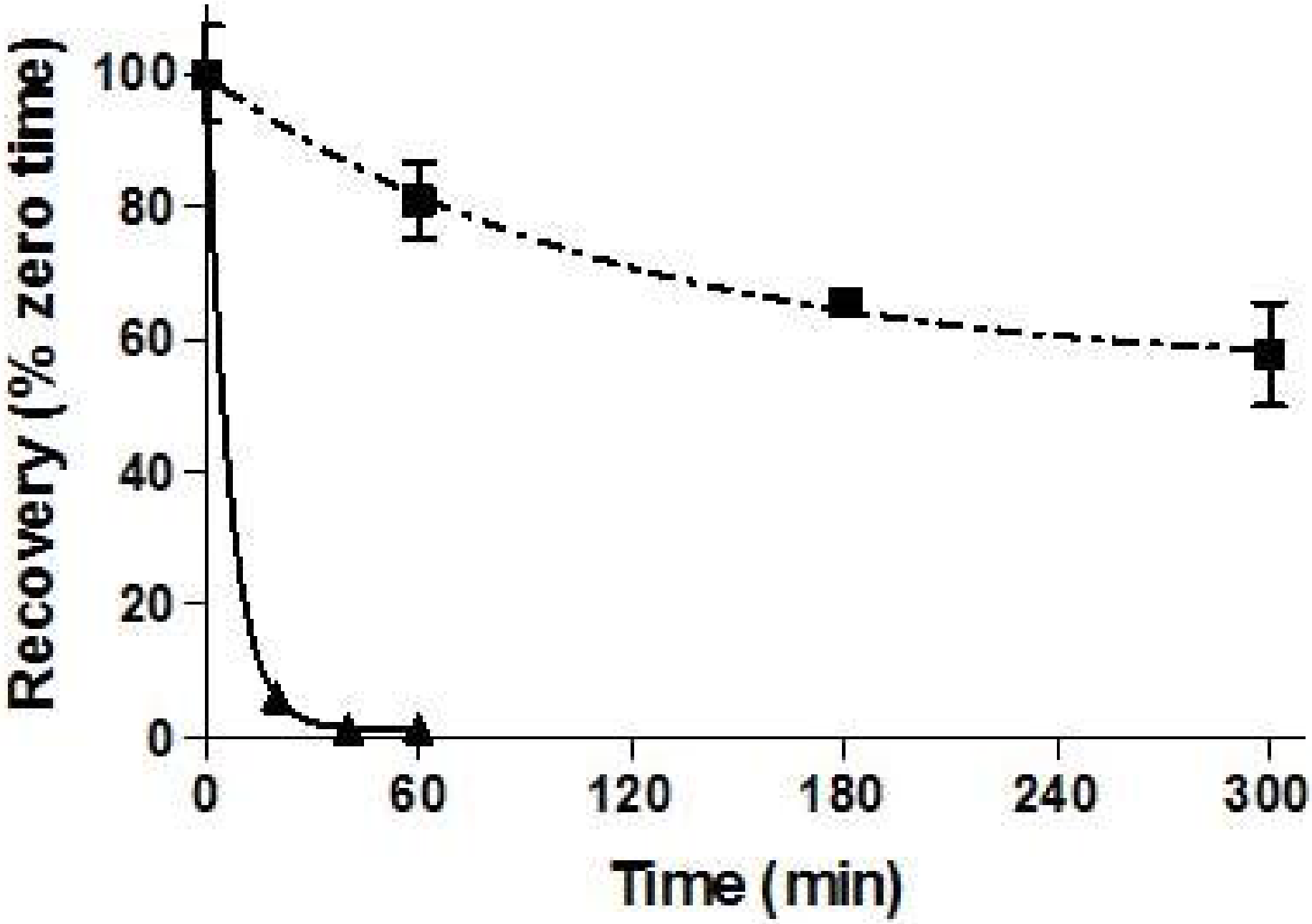
Recovery (% zero time)
100
80
60
40
20
0
0
60
120
180
240
300
Time (min)

Figure 1

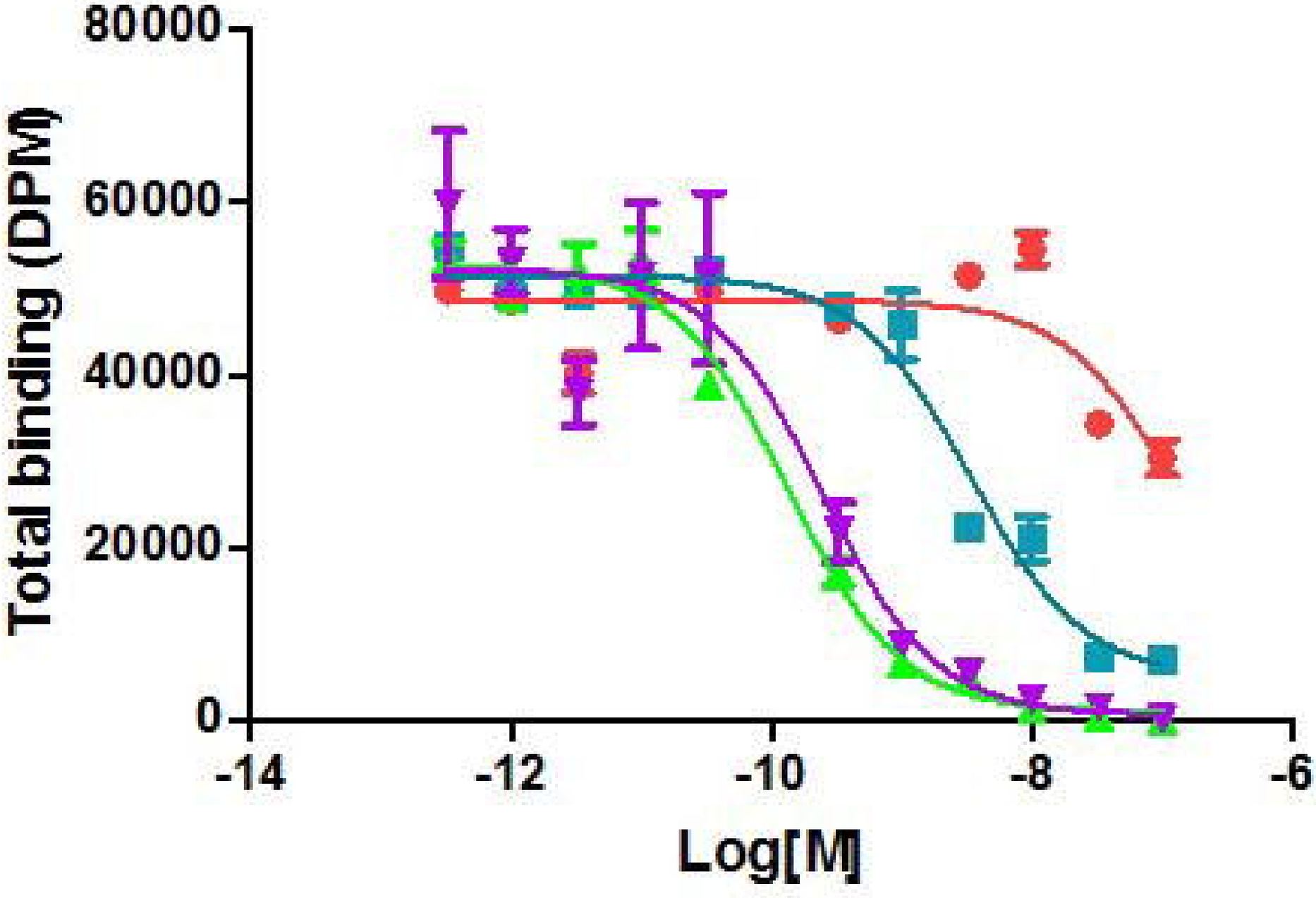

Figure 2

A.

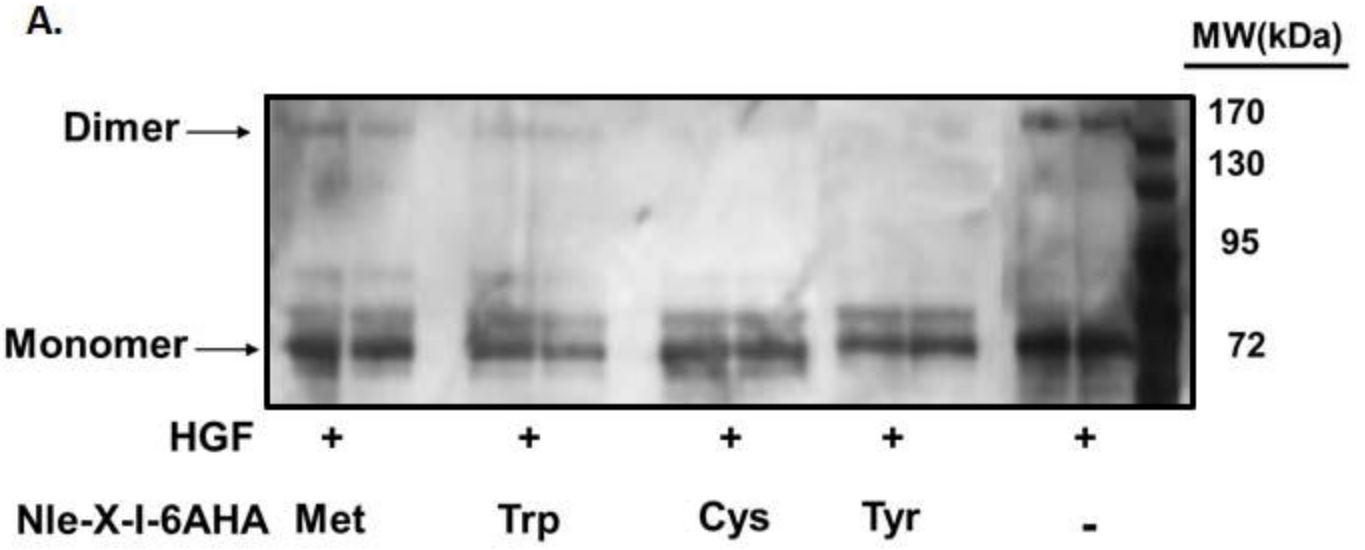
MW(kDa)
Dimer
Monomer
170
130
95
72
HGF + + + + +
Nle-X-I-6AHA Met Trp Cys Tyr -

B.

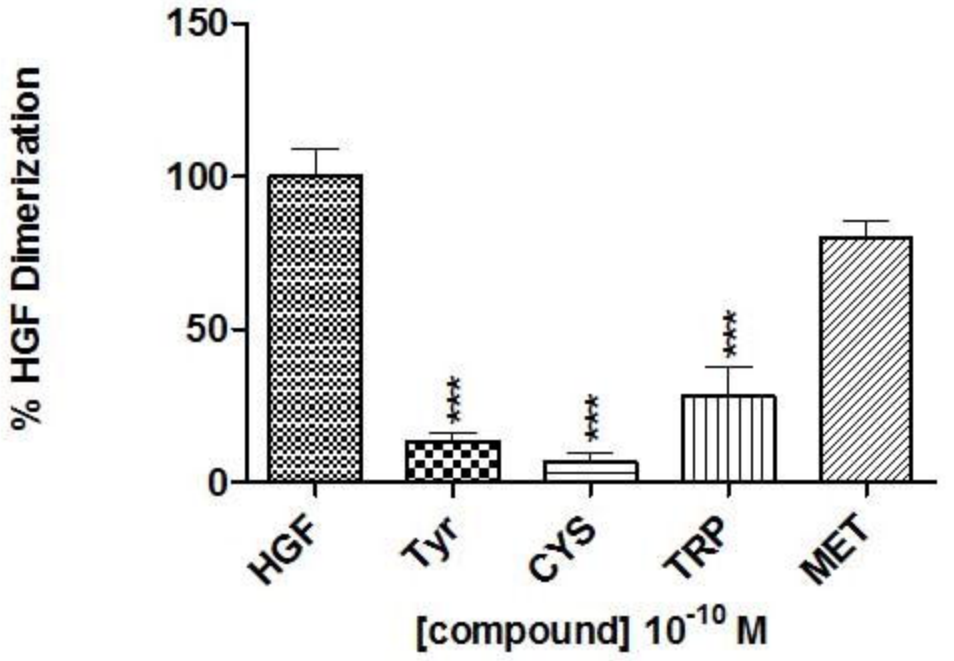
% HGF Dimerization
150
100
50
0
***
***
***
HGF
Tyr
CYS
TRP
MET
[compound] 10-10 M

Figure 3

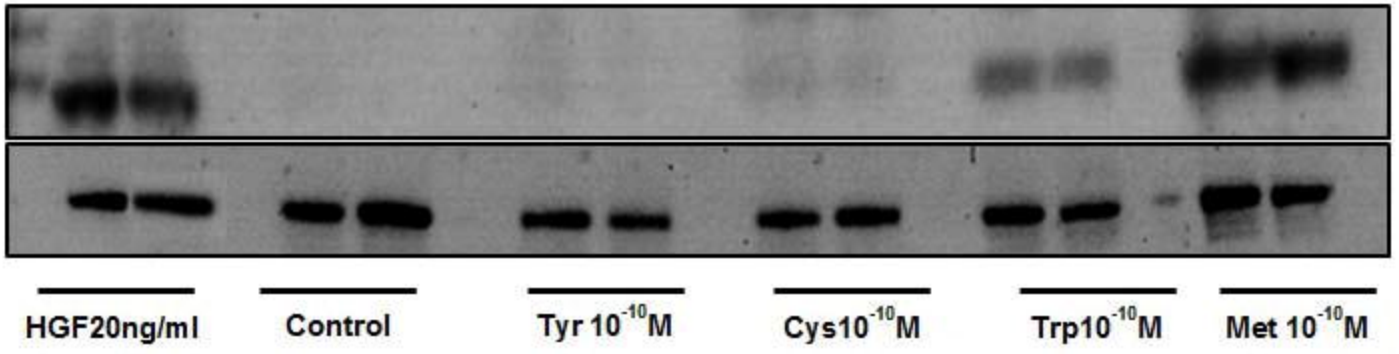

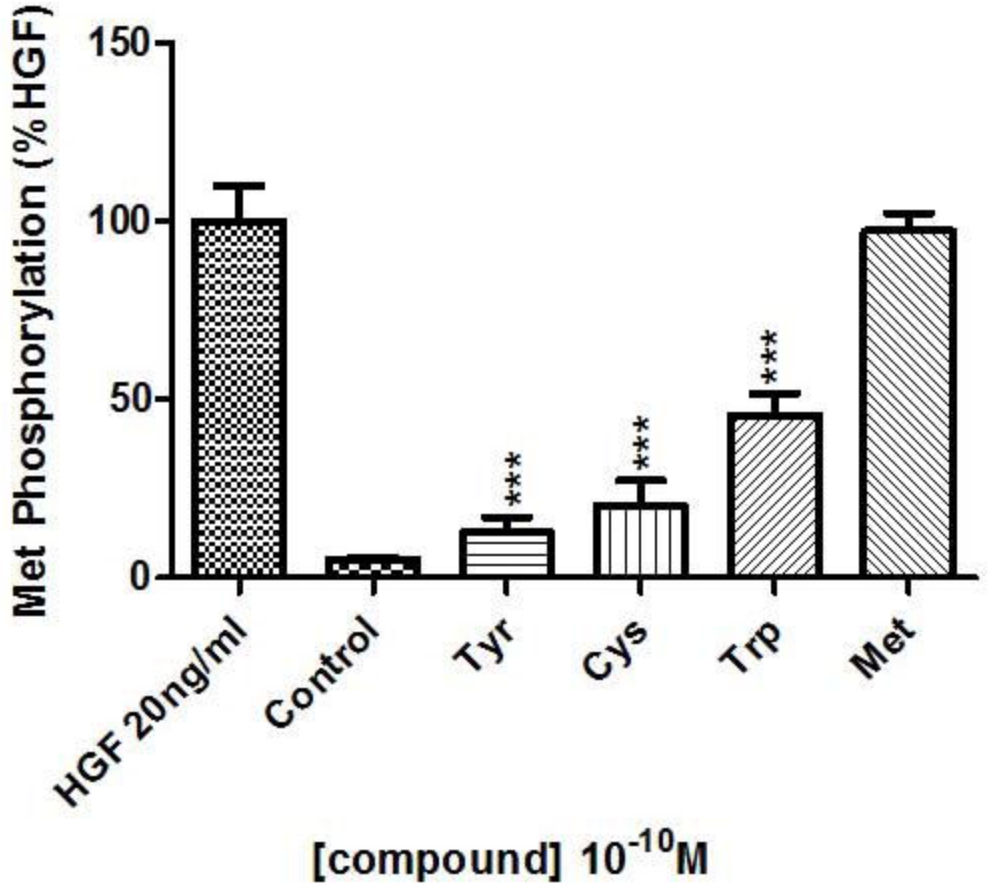

Figure 4

% HGF-dependent proliferation
150
100
50
0
-50
-100
-150
ns
***
**
ns
***
*
***
***
HGF 20ng/l
Control
Hinge 10-10M
Trp 10-10M
Met 10-10M
Asp 10-10M
Phe 10-10M
Ser 10-10M
Cys 10-10M
Tyr 10-10M
Treatment groups

Figure 5

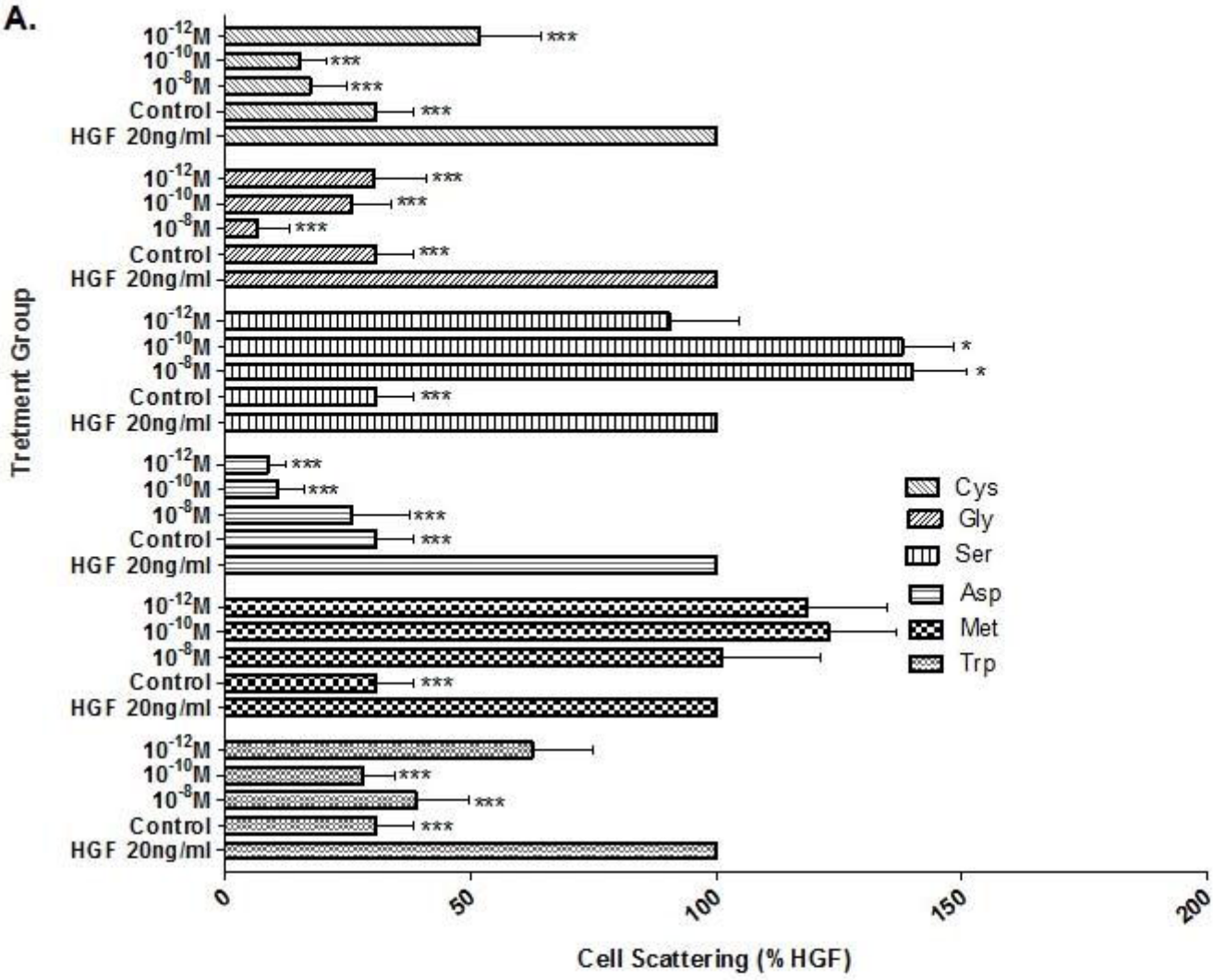
A.
Tretment Group
10-12M
10-10M
10-8M
Control
HGF 20ng/ml
***
*
Cys
Gly
Ser
Asp
Met
Trp
0
50
100
150
200
Cell Scattering (% HGF)

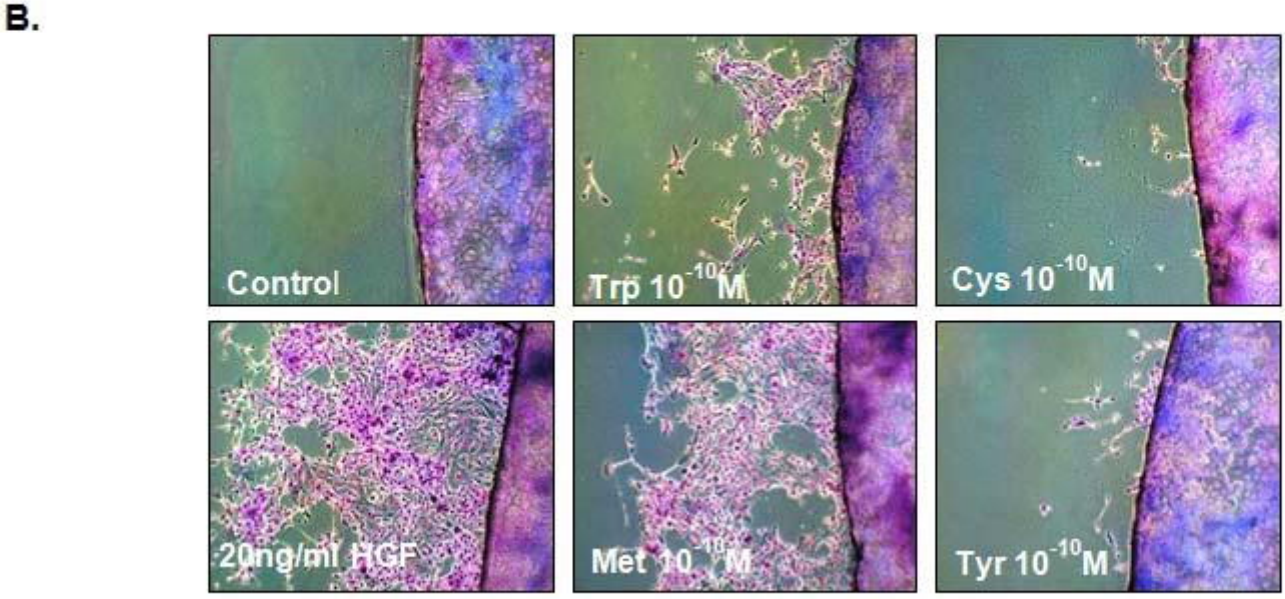
B.
Control
Trp 10-10M
Cys 10-10M
20ng/ml HGF
Met 10-10M
Tyr 10-10M

Figure 6

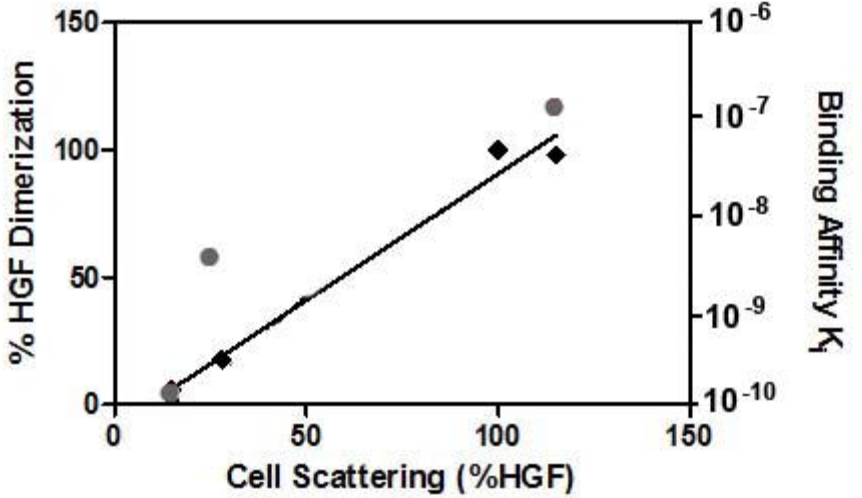
150
100
50
0
% HGF Dimerization
0
50
100
150
Cell Scattering (%HGF)
10 -6
10 -7
10 -8
10 -9
10 -10
Binding Affinity K

Figure 7

A.

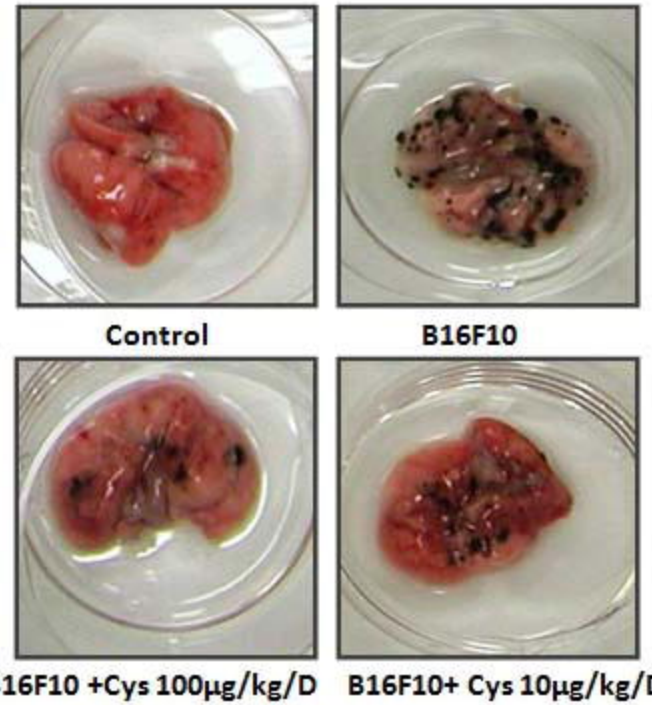
Control
B16F10
B16F10 +Cys 100µg/kg/D
B16F10+ Cys 10µg/kg/D

B.

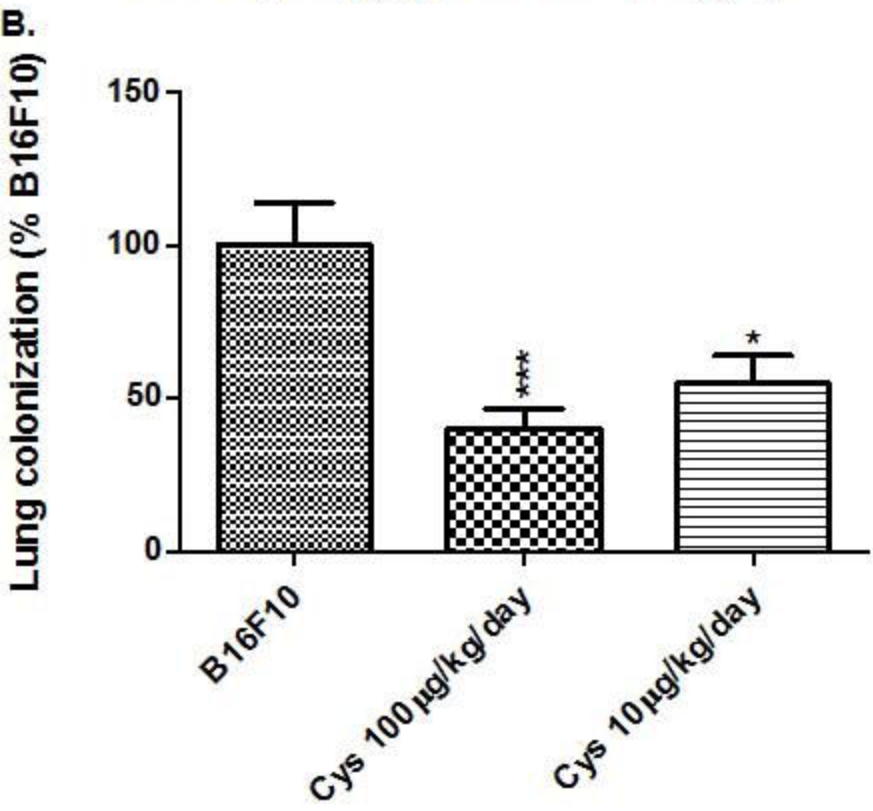
Lung colonization (% B16F10)
150
100
50
0
***
*
B16F10
Cys 100 µg/kg/day
Cys 10 µg/kg/day

Figure 8